Catal Lett (2008) 125:134–138
DOI 10.1007/s10562-008-9531-4

Origin of the High Activity and Stability of Co_3O_4 in Low-temperature CO Oxidation

Yong-Zhao Wang · Yong-Xiang Zhao · Chun-Guang Gao · Dian-Sheng Liu

Received: 20 April 2008 / Accepted: 27 May 2008 / Published online: 24 June 2008

Abstract In this paper, the Co_3O_4 catalysts prepared by the liquid phase precipitation method were investigated with respect to their activity and stability in CO oxidation reaction. The Co_3O_4 catalysts were comparatively investigated by thermal gravimetry analysis (TG-DTG), X-ray powder diffraction (XRD), N_2 adsorption, CO titration and O_2-temperature program desorption (O_2-TPD). The results of XRD show that all the catalysts exist as a pure Co_3O_4 phase with the spinel structure. The high catalytic activity observed at ambient temperature is followed by a gradual decrease. The CO titration experiments show that the Co_3O_4 catalysts possess active oxygen species. The total amount of active oxygen species and the specific surface area decrease with increasing calcination temperature. The O_2-TPD results indicate that O_2^- and O^- are the possible active oxygen species.

Keywords Co_3O_4 · Low-temperature CO oxidation · Catalytic activity · Active oxygen species

1 Introduction

The low-temperature catalytic oxidation of CO has become an important research topic over the years due to its many potential areas of applications. These applications include air-purification devices for respirator [1], pollution control devices for reducing industrial and automotive emissions [2], closed-cycle carbon dioxide lasers [3], carbon monoxide gas sensors [4, 5], removing trace quantities of CO from the ambient air in sealed cabins and fuel cell [6, 7]. Precious metal catalysts, such as Au/TiO_2, $Au/BaCO_3$, Au/ZrO_2, Au/CeO_2, Au/La_2O_3, $Au/CeO_2/Al_2O_3$, Pd/ZnO, Pd/CeO_2–TiO_2, Pd/CeO_2, Pt/CeO_2 and $Sn\text{-}Pt/SiO_2$, have been studied for CO oxidation and showed high activities [8–17]. Due to high prices and scarce of noble metal, attention has been given to search an alternative catalytic component to reduce using or even replace the noble metal. Transition metal oxides are good substitute catalysts because of their low-price and wide use [18–32]. Among them, cobalt oxide catalysts have attracted considerable attention because of their high catalytic activity for CO oxidation [25–32]. Up to now, the studies about CO oxidation over Co_3O_4 mainly focus on the preparation method of Co_3O_4 and the deactivation mechanism. However, the origin of high activity of Co_3O_4 in low-temperature CO oxidation is less studied.

The main purpose of the present work was to investigate the catalytic behavior and the origin of the high activity of the Co_3O_4 prepared via the liquid-precipitation method. CO oxidation was used as a test reaction.

2 Experimental

2.1 Preparation of Catalysts

The Co_3O_4 samples were prepared via a liquid-precipitation method in an aqueous solution. Thirty milliliters of 4.0 M cobalt nitrate solution was added drop by drop to 30 mL of 2.0 M ammonium acid carbonate solution under constant stirring at 25 °C. The temperature was then raised to 30 °C and maintained for 3 h. The final pH is about 8.0. The resulting suspension was filtered and the

Y.-Z. Wang · Y.-X. Zhao (✉) · C.-G. Gao · D.-S. Liu
School of Chemistry and Chemical Engineering, Engineering Research Center of Ministry of Education for Fine Chemicals, Shanxi University, Taiyuan 030006, China
e-mail: yxzhao@sxu.edu.cn

obtained precipitate was washed several times with deionized water, and then it was dried in air at 110 °C for 12 h. Finally, the samples were calcined at 300, 400 and 600 °C in flowing air for 3 h, respectively. The obtained samples were coded as LPC-T, where *T* refers to the calcination temperature.

2.2 Characterization of Catalysts

Thermal gravimetry analysis (TG/DTG) was carried out using a ZRY-1P thermal analyzer. The rate of heating was maintained at 10 °C/min and the mass of the sample was ~8 mg. The measurement was carried out from ambient temperature to 750 °C under nitrogen atmosphere flowing at a rate of 40 mL/min.

X-ray powder diffraction (XRD) analysis was performed to verify the species present in the catalysts. XRD patterns of the samples were recorded on a Rigaku D/MAX-RB X-ray diffractometer with a target of Cu K_α operated at 50 kV and 60 mA with a scanning speed of 0.5°/min and a scanning angle (2θ) range of 15–75°.

N_2 adsorption–desorption isotherms at −196 °C were determined using CE SORPTOMATIC 1990 SERIES instrument. Prior to the sorption experiments, the samples were degassed under vacuum at 150 °C for 12 h. The specific surface area (S_{BET}) was determined from the nitrogen adsorption isotherm.

The amount of active oxygen species on the catalysts was measured by CO titration at 25 °C. One hundred milligrams of sample was loaded in a 4 mm i.d. quartz microreactor and heated in flowing air (30 mL/min) at 300 °C for 30 min, then cooled to 25 °C in flowing N_2 (30 mL/min). One milliliter of 3%CO/N_2 was injected with a syringe repeatedly until no CO_2 was observed in the effluent gases. The time between the pulses was 5 min. The amount of active oxygen species was calculated from the amount of CO_2 obtained during the pulse. The analysis of the effluent gases (CO and CO_2) was performed with an on-line gas chromatograph equipped with a 3 m column packed with carbon molecular sieve, a methanator and a flame ionization detector (FID). In order to enhance the detection sensitivity, CO and CO_2 were converted to CH_4 by the methanator at 360 °C prior to entering into the FID. The minimum detection level was ca. 10 ppm.

The O_2-TPD investigation was performed in a conventional temperature programming system equipped with a TCD for analysis. The catalyst sample (100 mg) was pretreated in helium (99.995%) at 300 °C for 1 h, then the oxygen adsorption was proceeded with 20%O_2/N_2 at 200 °C for 0.5 h. After cooling to room temperature, the O_2-TPD measurement was performed using helium (30 mL/min) as carrier gas. The temperature was increased at a rate of 15 °C/min from room temperature to 900 °C.

2.3 Measurement of Catalytic Activity

The measurements of catalytic activity of low-temperature CO oxidation were carried out in a continuous flow laboratory microreactor under atmospheric pressure. The microreactor was a 8 mm i.d. quartz u-tube, and a thermocouple enveloped in glass was set into the catalyst bed to measure the temperature. The samples were sieved to 40–60 mesh so that pressure drop and concentration and temperature gradients over the catalyst bed were negligible. Three hundred milligrams of catalyst was used for each run. The feed gases adjusted by mass flow controllers consisted of 0.5 vol% CO, 14.4 vol% O_2 and 85.1 vol% N_2 passed through the catalyst bed with a total flow rate of 20 mL/min. Quantitative analysis of CO and CO_2 was the same as the method described in the CO titration experiment. Prior to all catalytic experiments the catalysts were pretreated in flowing air at 300 °C for 30 min to yield clean surface and then cooled to room temperature in the absence of flowing air. During the test, pretreatment and reaction gases were dried fully through the molecular sieve and silica gel.

The CO conversion was calculated based on the CO consumption as follows:

$$\%\ \text{of conversion of CO} = \frac{[\text{CO}]_{\text{in}} - [\text{CO}]_{\text{out}}}{[\text{CO}]_{\text{in}}} \times 100$$

3 Results and Discussion

3.1 TG-DTG Analysis of Co_3O_4

Figure 1 shows the TG-DTG curves for the decomposition of Co_3O_4 precipitate dried at 80 °C in a dynamic nitrogen (40 mL/min) environment. The TG curve shows the two weight loss steps and the DTG curve shows the maximum

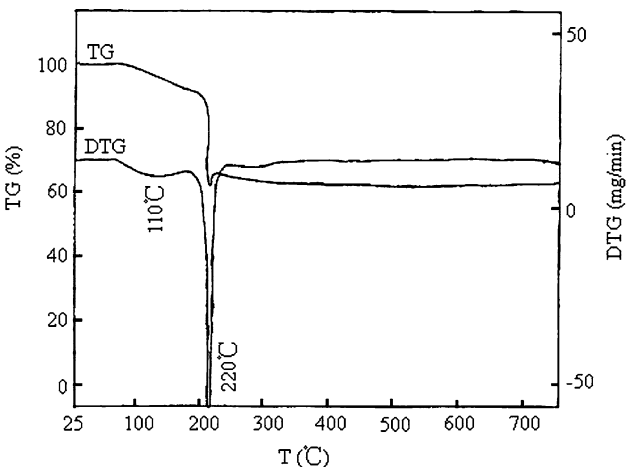

Fig. 1 The TG-DTG curves of Co_3O_4 dried at 80 °C

loss rate at 110 and 220 °C (labeled as T_1 and T_2), respectively. Weight loss of 8.4% in T_1 step is mainly the removal of the surface adsorbed water. Weight loss of 31.6% in T_2 should be the decomposition of $Co_2(OH)_2CO_3$ into Co_3O_4 that is close to the theoretical value (35.4%). No obvious weight loss was observed above 300 °C. Therefore, the results indicate that Co_3O_4 calcined at 300 °C or higher temperatures becomes stable.

3.2 XRD and S_{BET} Analysis of Co_3O_4

The XRD patterns of a series of Co_3O_4 catalysts obtained at different calcination temperatures are presented in Fig. 2. Powder XRD peaks of the cobalt oxide are well consistent with the data of the JCPDS file of Co_3O_4 with cubic phase. The peaks at 2θ value of 18.9°, 31.2°, 36.9°, 38.6°, 44.8°, 55.6°, 59.3° and 65.2° correspond to the crystal planes of (111), (220), (311), (222), (400), (422), (511) and (440) of crystalline Co_3O_4, respectively. It is clear that Co_3O_4 is the only phase after the decomposition of the precipitate at 300, 400 and 600 °C, and no diffraction peak other than those of Co_3O_4 are present. All the samples are well crystallized and the degree of crystallinity increases gradually with increasing the calcination temperature. It is seen that LPC-300 diffraction peaks (Fig. 2a) are broader and lower than others, indicating the presence of very small crystal size of Co_3O_4. However, the diffraction peaks of LPC-600 become sharper apparently (Fig. 2c), and the sample LPC-400 is position medium.

The average particle sizes of the Co_3O_4 calcined at different temperature, according to the (311) diffraction pattern of crystalline Co_3O_4, can be calculated using the well-known Scherrer equation [34]. From the calculational results it can be seen that the order of the particle size is: LPC-600(62 nm) > LPC-400(20 nm) > LPC-300(10 nm).

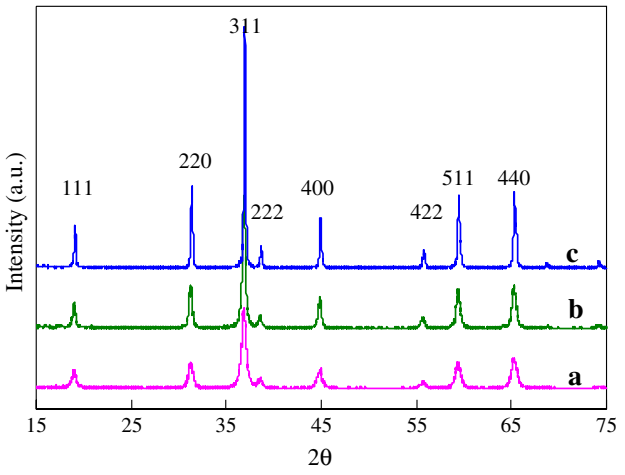

Fig. 2 XRD patterns of Co_3O_4 calcined at different temperatures: (**a**) 300 °C; (**b**) 400 °C; (**c**) 600 °C

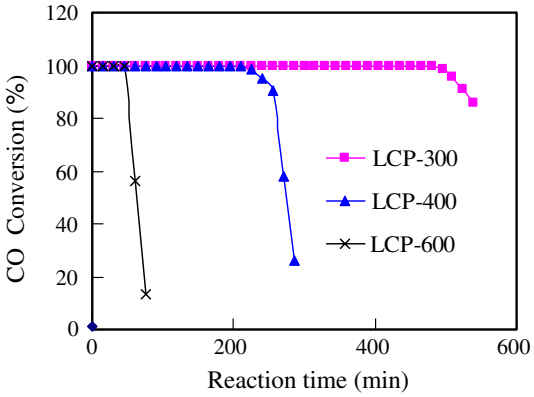

Fig. 3 The catalytic performance of the catalysts calcined at different temperatures

However, the order of S_{BET} of the Co_3O_4 catalysts is: LPC-300(54 m^2 g^{-1}) > LPC-400(30 m^2 g^{-1}) > LPC-600(9 m^2 g^{-1}), which is opposite to that of the particle size. The decrease of the S_{BET} is probably due to the growth and aggregation of the Co_3O_4 nanoparticles with the increasing calcinations temperature.

3.3 Activity Measurement

The relationships between CO oxidation performance and reaction time on various catalysts are shown in Fig. 3. Figure 3 indicates that the LPC-300, LPC-400 and LPC-600 exhibit very high catalytic activity at room temperature and the calcination temperature has a strong influence on the catalytic performance. The reaction stability increases gradually with the decrease of calcination temperature. The time of CO complete conversion is 50, 230 and 500 min, respectively.

3.4 CO Titration Analysis

From the results of XRD, S_{BET} analysis and the activity measurement, it can be seen that the time of CO complete conversion is related to the particle size and the surface specific area, however, which could not simply elucidate the low-temperature high activity of the Co_3O_4 catalyst. There maybe is the surface oxygen species that affects the catalytic performance [35].

In order to study the origin of high activity of the Co_3O_4 in low-temperature CO oxidation, CO titration analysis was performed and the results were summarized in Figs. 4 and 5. It is clear that all the Co_3O_4 catalysts produce CO_2 at ambient temperature in a similar manner, in the absence of gas phase oxygen. It indicates that the active oxygen species formed during the pretreatment process on the catalysts can react with the CO at ambient temperature. From Fig. 4 we can also see that CO can be oxidized

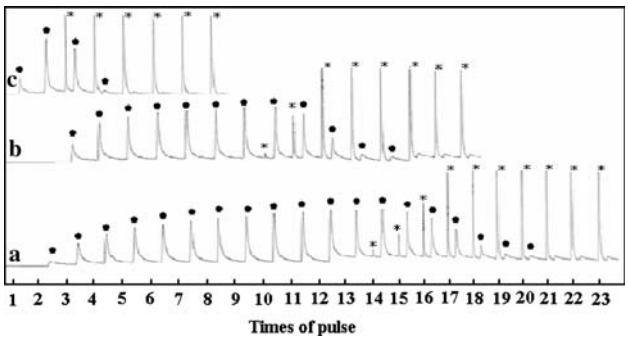

Fig. 4 CO titration reaction over Co_3O_4 catalysts (25 °C, *-CO, ●-CO_2) (**a**)-LPC-300, (**b**)-LPC-400, (**c**)-LPC-600

completely over LPC-300 in the thirteenth pulse. However, over LPC-600, CO cannot be converted completely in the third pulse. According to the amount of CO_2 obtained during the pulse, the amount of active oxygen species can be calculated. The relationships between the amount of active oxygen species and calcination temperature are shown in Fig. 5. With increase of calcination temperature, the amount of active oxygen species over the catalysts also decreases, which is one of the main factors that affects the catalytic stability.

3.5 O_2-TPD

The results of CO titration analysis show that the all the catalysts possess active oxygen species, and the amount of the active oxygen species have largely depended on the calcination temperature.

To investigate the type of oxygen species and identify the active oxygen species, the samples were pretreated in helium (99.995%) at 300 °C for 1 h, and the oxygen adsorption was proceeded with 20%O_2/N_2 at 200 °C for 0.5 h, then they were used for O_2-TPD measurement. Figure 6 shows the O_2-TPD profiles of the samples. At least four kinds of oxygen species desorb, which are

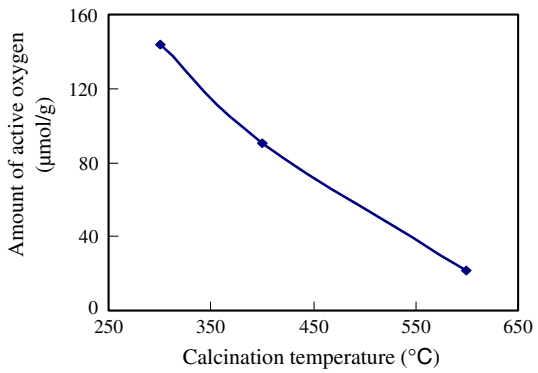

Fig. 5 Effect of calcination temperature on the amount of active oxygen species

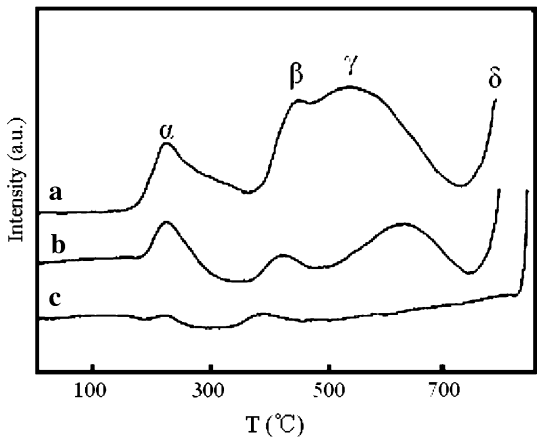

Fig. 6 The O_2-TPD profiles of the samples (**a**)-LPC-300, (**b**)-LPC-400, (**c**)-LPC-600

designated as peaks α, β, γ and δ, respectively. As shown in the figure, peak α is located at about 225 °C and with calcination temperature increasing the area of the peak decrease gradually. However, the temperatures of peak β are at 390, 420 and 440 °C, respectively. The temperatures of peak γ increase with the calcination temperature increasing.

Generally, the adsorbed oxygen changes by the following procedures: $O_2(ad) \rightarrow O_2^-(ad) \rightarrow O^-(ad) \rightarrow O^{2-}(lattice)$ [36]. The physically adsorbed oxygen and $O_2^-(ad)$ species are relatively easy to desorb. In Fig. 6 peak α may be $O_2^-(ad)$ species. The temperature of β and γ peak are relatively high, therefore, it is more reasonable to assign them to the desorption of O^- species. Besides the three peaks, there is another one at very high temperature (>700 °C), which perhaps comes from the lattice oxygen. Figure 7 is the O_2-TPD profiles of the fresh and deactivated catalyst (LPC-400). From the figure we can see that after deactivation the peak

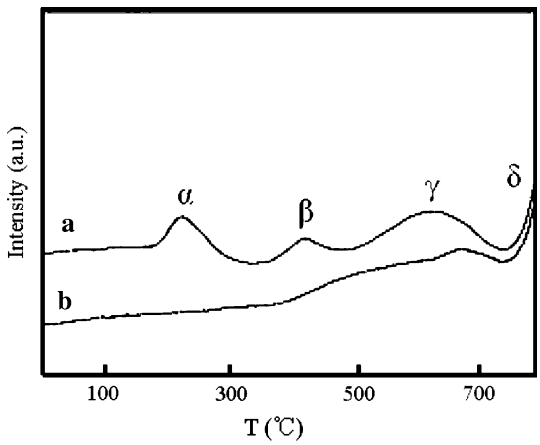

Fig. 7 The O_2-TPD profiles of the fresh and deactivated samples (**a**) the fresh, (**b**) the deactivated

α and β and part of the peak γ disappear, but the peak δ is same as the fresh. So we can concluded that O_2^- and O^- are the possible active oxygen species, however, the lattice oxygen has no effect on the activity and stability of the catalyst in low-temperature CO oxidation.

4 Conclusions

The Co_3O_4 catalysts have been prepared by the liquid phase precipitation method and calcined at different temperatures. All samples exist as a pure Co_3O_4 phase with the spinel structure. These catalysts exhibit high catalytic activities toward the oxidation of CO at low temperature. The CO titration experiments show that the Co_3O_4 catalysts possess active oxygen species, which is the origin of high activity. The total amount of the active oxygen species and the specific surface area decrease with increasing calcination temperature. According to the O_2-TPD results of the fresh and the deactivated samples, we determine the O_2^- and O^- species responsible for the possible active oxygen species. The lattice oxygen has no effect on the catalytic performance of Co_3O_4 in low-temperature CO oxidation.

Acknowledgments The authors thank the Shanxi Natural Science Foundation (grants: 20041017) and Shanxi Scientific & Technological Promoted Project of China (grants: 031099) for the financial support of this work.

References

1. Lamb AB, Bray WC, Frazer JCW (1920) Ind Eng Chem 12:213
2. Thormählen P, Fridell E, Cruise N, Skoglundh M, Palmqvist A (2001) Appl Catal B 31:1
3. Tripathi AK, Gupta NM, Chatterji UK, Iyer RM (1992) Indian J Technol 30:107
4. Yamaura H, Moriya K, Miura N, Yamazoe N (2000) Sens Actuators B 65:39
5. Funazaki N, Asano Y, Yamashita S, Kobayashi T, Haruta M (1993) Sens Actuators B 13–14:536
6. Kim DH, Lim MS (2002) Appl Catal A 224:27
7. Snytnikov PV, Sobyanin VA, Belyaev VD, Tsyrulnikov PG, Shitova NB, Shlyapin DA (2003) Appl Catal A 239:149
8. Lian HL, Jia MJ, Pan WC, Li Y, Zhang WX, Jiang DZ (2005) Catal Commun 6:47
9. Soares JMC, Bowker M (2005) Appl Catal A 291:136
10. Glaspell G, Fuoco L, El-Shall MS (2005) J Phys Chem B 109:17350
11. Fierro-Gonzalez JC, Bhirud VA, Gates BC (2005) Chem Commun 5275
12. Centeno MÁ, Portales C, Carrizosa I, Odriozola JA (2005) Catal Lett 102:289
13. Moreau F, Bond GC (2006) Catal Today 114:362
14. Luo MF, Hou ZY, Yuan XX, Zheng XM (1998) Catal Lett 50:205
15. Dong GL, Wang JG, Gao YB, Chen SY (1999) Catal Lett 58:37
16. Bera P, Gayen A, Hegde MS, Lalla NP, Spadaro L, Frusteri F, Arena F (2003) J Phys Chem B 107:6122
17. Margitfalvi JL, Borbáth I, Hegedűs M, Tfirst E, Gőbölös S, Lázár K (2000) J Catal 196:200
18. Luo MF, Zhong YJ, Yuan XX, Zheng XM (1997) Appl Catal A 162:121
19. Hutchings GJ, Mirzaei AA, Joyner RW, Siddiqui MRH, Taylor SH (1998) Appl Catal A 166:143
20. Taylor SH, Hutchings GJ, Mirzaei AA (1999) Chem Commun 1373
21. Whittle DM, Mirzaei AA, Hargreaves JSJ, Joyner RW, Kiely CJ, Taylor SH, Hutchings GJ (2002) Phys Chem Chem Phys 4:5915
22. Bae CM, Ko JB, Kim DH (2005) Catal Commun 6:507
23. Huang J, Wang SR, Zhao YQ, Wang XY, Wang SP, Wu SH, Zhang SM, Huang WP (2006) Catal Commun 7:1029
24. Yang XM, Luo LT, Zhong H (2005) Catal Commun 6:13
25. Yu Y, Yung F (1974) J Catal 33:108
26. Jia MJ, Zhang WX, Tao YG, Wang GY, Cui XH, Zhang CL, Wu TH (1999) Chem J Chin Univ (in Chinese) 20:637
27. Lin HK, Chiu HC, Tsai HC, Chien SH, Wang CB (2003) Catal Lett 88:169
28. Lin HK, Wang CB, Chiu HC, Chien SH (2003) Catal Lett 86:63
29. Wang CB, Tang CW, Gau SJ, Chien SH (2005) Catal Lett 101:59
30. Cunningham DAH, Kobayashi T, Kamijo N, Haruta M (1994) Catal Lett 25:257
31. Jansson J (2000) J Catal 194:55
32. Jansson J, Palmqvist AEC, Fridell E, Skoglundh M, Österlund L, Thormählen P, Langer V (2002) J Catal 211:387
33. Wang YZ, Zhao YX, Gao CG, Liu DS (2007) Catal Lett 116:136
34. Langford JI, Wilson AJC (1978) J Appl Crystallogr 11:102
35. Davies TE, García T, Solsona B, Taylor SH (2006) Chem Commun 3417
36. Bielan'ski A, Haber J (1979) Catal Rev-Sci Eng 19:1